Tree Physiology 28, 1609–1617

Constraints on physiological function associated with branch architecture and wood density in tropical forest trees

FREDERICK C. MEINZER,[1,2] PAULA I. CAMPANELLO,[3] JEAN-CHRISTOPHE DOMEC,[4] M. GENOVEVA GATTI,[3] GUILLERMO GOLDSTEIN,[3,5] RANDOL VILLALOBOS-VEGA[5] and DAVID R. WOODRUFF[1]

[1] *USDA Forest Service, Pacific Northwest Research Station, Corvallis, OR 97331, USA*

[2] *Corresponding author (fmeinzer@fs.fed.us)*

[3] *Laboratorio de Ecología Funcional, Departamento de Ecología, Genética y Evolución, Facultad de Ciencias Exactas y Naturales, Universidad de Buenos Aires, Buenos Aires (C1428EHA), Argentina*

[4] *Department of Forestry and Environmental Resources, North Carolina State University, Raleigh, NC 27695, USA*

[5] *Department of Biology, University of Miami, Coral Gables, FL 33124, USA*

Received June 3, 2008; accepted August 1, 2008; published online September 2, 2008

Summary This study examined how leaf and stem functional traits related to gas exchange and water balance scale with two potential proxies for tree hydraulic architecture: the leaf area:sapwood area ratio (A_L:A_S) and wood density (ρ_w). We studied the upper crowns of individuals of 15 tropical forest tree species at two sites in Panama with contrasting moisture regimes and forest types. Transpiration and maximum photosynthetic electron transport rate (ETR_{max}) per unit leaf area declined sharply with increasing A_L:A_S, as did the ratio of ETR_{max} to leaf N content, an index of photosynthetic nitrogen-use efficiency. Midday leaf water potential, bulk leaf osmotic potential at zero turgor, branch xylem specific conductivity, leaf-specific conductivity and stem and leaf capacitance all declined with increasing ρ_w. At the branch scale, A_L:A_S and total leaf N content per unit sapwood area increased with ρ_w, resulting in a 30% increase in ETR_{max} per unit sapwood area with a doubling of ρ_w. These compensatory adjustments in A_L:A_S, N allocation and potential photosynthetic capacity at the branch level were insufficient to completely offset the increased carbon costs of producing denser wood, and exacerbated the negative impact of increasing ρ_w on branch hydraulics and leaf water status. The suite of tree functional and architectural traits studied appeared to be constrained by the hydraulic and mechanical consequences of variation in ρ_w.

Keywords: capacitance, functional convergence, hydraulic architecture, osmotic potential, photosynthesis, transpiration, water potential.

Introduction

Because the integrity and efficiency of long-distance water transport are critical to the growth and survival of land plants, especially trees, fundamental features constraining hydraulic architecture are expected to play a dominant role in determining a broad range of functional traits. Whole-plant leaf area-specific conductance (K_l) is a higher order component of hydraulic architecture that integrates the hydraulic properties of the entire soil-to-leaf water transport pathway (Küppers 1984). As an index of the efficiency of water supply in relation to potential transpirational demand, K_l is expected to constrain stomatal control of leaf gas exchange and water balance (Meinzer 2002, Sperry et al. 2002), and a number of studies have reported a close coordination between K_l and leaf gas exchange both within (Meinzer and Grantz 1990, Hubbard et al. 2001) and across (Meinzer et al. 1995, Mencuccini 2003, Santiago et al. 2004, Campanello et al. 2008) species. Similarly, the leaf area to sapwood area ratio (A_L:A_S) is a tree architectural index of potential transpirational demand relative to water transport capacity and therefore a potential proxy for K_l (Andrade et al. 1998, Tausend et al. 2000, Bucci et al. 2005).

In diffuse-porous species, variation in wood density (ρ_w) should constrain stem hydraulics (Stratton et al. 2000) because ρ_w is an index of the balance between solid material and the relative cross-sectional area available for water transport. Plant functional traits shown to be inversely related to ρ_w include rates of leaf gas exchange (Bucci et al. 2004, Santiago et al. 2004), xylem-specific and leaf-specific conductivity (Stratton et al. 2000, Bucci et al. 2004, Santiago et al. 2004), minimum leaf water potential (Bucci et al. 2004, Santiago et al. 2004), leaf osmotic potential at the turgor loss point (Gartner and Meinzer 2005), xylem vulnerability to embolism and implosion (Hacke et al. 2001) and xylem hydraulic capacitance (Meinzer et al. 2003, Pratt et al. 2007, Scholz et al. 2007).

Because multi-species surveys involving measurement of hydraulics in intact, field-grown plants present a series of methodological and logistical difficulties associated with simultaneous measurements of water fluxes and their driving forces, both of which are rarely steady state (Goldstein et al. 1998, Andrade et al. 1998, Domec et al. 2007), the ability to

link higher order functional traits to tree architectural features and biophysical properties that are relatively simple to measure would be beneficial. Nevertheless, relatively few studies have examined the extent to which higher order functional traits and physiological regulatory behavior scale in a species-independent manner with basic structural and biophysical attributes that govern hydraulic architecture. Correlations among traits may not necessarily be indicative of the mechanisms driving the relationships, but comparisons of multiple relationships across a range of organization from the simplest physical traits to more complex functional traits are likely to suggest potential mechanisms underlying the scaling relationships observed.

We studied individuals of 15 tropical forest tree species at two sites in Panama with contrasting rainfall regimes and forest types to examine how a number of leaf, stem and branch level functional traits related primarily to gas exchange and water balance scale with A_L:A_S and ρ_w of upper canopy branches. For the reasons outlined above, A_L:A_S and ρ_w are potential surrogates for various aspects of tree hydraulic architecture that should provide a basis for drawing inferences concerning the mechanistic nature of the leaf- and branch-level scaling relationships observed. We hypothesized that scaling relationships would be driven by the impacts of variation in A_L:A_S and ρ_w on hydraulic architecture and water balance. Specifically, we expected to observe inverse relationships between A_L:A_S and indices of leaf gas exchange capacity because A_L:A_S is a potential architectural proxy for K_l. As such, increasing A_L:A_S would imply decreasing water supply in relation to demand. In addition, we predicted that xylem specific conductivity and hydraulic capacitance would be inversely related to ρ_w and that these inverse relationships would be associated with greater fluctuations in leaf water status in species with denser wood.

Materials and methods

Study sites and plant material

Data were collected during the dry seasons of 1994, 1996, 2000, 2001, 2003 and 2004 from two canopy cranes operated by the Smithsonian Tropical Research Institute (STRI) in the Republic of Panama. Each crane is equipped with a gondola suspended by cables from a rotating jib that allows access to about 0.8 ha of forest. One crane is located in an old-growth forest in the Parque Nacional San Lorenzo on the Caribbean side of the Isthmus of Panama, where mean annual precipitation is about 3100 mm. The other crane is located in a seasonally dry secondary forest in the Parque Natural Metropolitano near the edge of Panama City, which receives about 1800 mm of precipitation annually, with a distinct dry season between late December and April. The dry season at Parque San Lorenzo is shorter and less intense that at Parque Metropolitano. There is no overlap among tree species between the two sites. Seven individuals were studied at the Parque San Lorenzo site and eight at the Parque Metropolitano site representing a total of 15 species (Table 1).

Transpiration

The constant heating method described by Granier (1985) was used to measure transpiration (E) as sap flow through branches in the upper crowns of 12 species. For measurements in 1996, a pair of 20-mm-long, 2-mm-diameter temperature probes (UP GmbH, Munich, Germany) was installed in each of three to four replicate branches per tree. The upper (downstream) probe was continuously heated with a constant current power supply (UP GmbH), while the unheated upstream probe served as a temperature reference. For measurements in 2000, 2001 and 2004, variable length probes with a heated and

Table 1. Characteristics of the individual trees studied at two tropical forest sites in Panama.

Species	Family	Diameter (m)	Height (m)	A_L:A_S (m^2 cm^{-2})	Wood density (g cm^{-3})
Parque San Lorenzo					
Aspidosperma cruenta	Apocynaceae	0.29	29	1.16	0.74
Manilkara bidentata	Sapotaceae	0.66	30	0.61	0.67
Protium panamense	Burseraceae	0.28	16	0.58	0.62
Tachigalia versicolor	Fabaceae	0.31	23	1.19	0.64
Tapirira guianensis	Anacardiaceae	0.70	34	0.67	0.50
Trattinickia aspera	Burseraceae	0.37	24	0.64	0.57
Vochysia ferruginea	Vochysiaceae	0.42	26	0.72	0.56
Mean		0.43	26	0.80	0.61
Parque Metropolitano					
Anacardium excelsum	Anacardiaceae	0.98	38	0.51	0.39
Cecropia longipes	Cecropiaceae	0.20	18	0.34	0.33
Chrysophyllum cainito	Sapotaceae	0.33	23	0.90	0.66
Cordia alliodora	Boraginaceae	0.34	26	0.65	0.52
Ficus insipida	Moraceae	0.65	28	0.50	0.40
Luehea seemannii	Tiliaceae	0.75	24	0.58	0.48
Schefflera morototoni	Araliaceae	0.47	22	0.45	0.40
Spondias mombin	Anacardiaceae	0.33	23	0.39	0.38
Mean		0.51	25	0.54	0.44

reference sensor measuring length of 10 mm at the probe tip (James et al. 2002) were installed in three to five replicate branches per tree. All probes were shielded with a layer of foam insulation surrounded by an outer layer of reflective insulation. Concurrent differential voltage measurements across the copper thermocouple leads were converted to a temperature difference between the heated and reference sensor (ΔT). Signals from the sap flow probes were scanned every minute and 10-min means were recorded by a data logger equipped with a 32-channel multiplexer and stored in a solid-state storage module. Mass flow of sap was obtained by multiplying flow density by the sapwood area, which included the entire cross-sectional area of the xylem for the size range of branches in which probes were installed (3 to 6-cm-diameter). Leaf area distal to the probes ranged from 2 to 13 m^2 and was determined by multiplying the total number of leaves by the mean area per leaf obtained from a subsample of 50 to 200 leaves.

Photosynthetic capacity and leaf nitrogen content

Chlorophyll fluorescence was measured on 10 species during 2003 using a pulse-amplitude modulated yield analyzer (Mini-PAM, Waltz, Effeltrich, Germany). Saturation pulses were applied for 0.8 s at a photosynthetic photon flux (PPF) of 3500 μmol m^{-2} s^{-1}. Measurements were made between predawn and midday in fully expanded and exposed sun leaves to minimize the impacts of any afternoon depression in photosynthetic capacity or photoinhibition associated with acclimation to shade. Quantum yields of PS II were obtained for the complete range of PPF values experienced by plants (0 to 2000 μmol m^{-2} s^{-1}). Measurements of PPF were made with the Mini-PAM's micro-quantum sensor. A steady-state light response curve for each species was generated with leaves adapted to the PPF values measured in the field. Maximum fluorescence yield (F_m) and dark fluorescence yield (F_o) of PSII were recorded in predawn conditions to determine dark-adapted quantum yields ($F_v/F_m = F_m - F_o)/F_m$). Dark-adapted quantum yield corresponded to the initial points of the light curves. Steady-state fluorescence (F) and maximal fluorescence in the light-adapted state (F_m') of PSII were measured for different PPF values. Values of electron transport rates (ETR) through PSII were obtained from quantum yield ($\Delta F/F_m' = (F_m' - F)/F_m'$):

$$\mathrm{ETR} = (\Delta F/F_m')\, I\, \alpha\, 0.5 \quad (1)$$

where I is the incident PPF, and α is leaf absorbance. The 0.5 factor assumes an even distribution of absorbed quanta between PSII and PSI so two photons are required per electron passed through PSII. The ETR correction factor "α" takes into account that only a fraction of incident light is absorbed by the two photosystems. A value of $\alpha = 0.84$ was used for calculations (Ehleringer 1981, Björkman and Demmig 1987).

The photosynthetic capacity expressed as the maximum electron transport rate ($\mathrm{ETR_{max}}$; μmol electrons m^{-2} s^{-1}) was calculated from light curves using the asymptotic exponential equation:

$$y = (\mathrm{ETR_{max}})\,(1 - e^{-bx}) \quad (2)$$

where y is photosynthetic rate, x is irradiance and b is the instantaneous fractional growth rate of the exponential function (Rascher et al. 2000). Curve fits obtained with this equation yielded r^2 values ranging from 0.87 to 0.99, consistent with the absence of significant photoinhibition.

Foliage on which chlorophyll fluorescence was measured was collected, dried and ground and analyzed for N content on a Carlo Erba elemental analyzer (NC 2500, CE Elantech, Lakewood, NJ). For the remaining five species, total N content of fully exposed upper canopy leaves was determined by the micro-Kjeldahl method. Leaf mass per area (LMA) was determined on a minimum of five leaves per species.

Leaf water relations

The water potential of upper-canopy leaves (Ψ_L) of nine species was determined with a pressure chamber (PMS Instrument Company, Albany, OR) near midday on clear dry days during the dry season. At each sampling time, measurements were obtained from three to five leaves of each tree. Balance pressures were determined either in the canopy crane gondola immediately after leaf excision, or the leaves were sealed in plastic bags and dropped to the base of the crane for determination of balance pressures within 10 min of excision.

The pressure–volume technique (Tyree and Hammel 1972) was used to assess bulk leaf osmotic potential at zero turgor ($\Psi_{\pi z}$) and leaf capacitance (C) in nine of the species. Portions of terminal branches were excised in the upper canopy and their bases immediately recut under water. The cut ends remained under water with the terminal leafy portions enclosed in a plastic bag to allow partial rehydration during transit from the canopy crane to the laboratory. Individual leaves or leafy shoots were used for pressure–volume analyses depending on petiole length and leaf size. Pressure–volume curves were initiated by first determining the fresh mass of the sample, then measuring its water potential with a pressure chamber. Alternate measurements of fresh mass and Ψ_L were repeated during slow dehydration on the laboratory bench until Ψ_L approached the measuring range of the pressure chamber (−4 MPa). We tested for rehydration-induced artifacts previously reported for some woody species (Bowman and Roberts 1985, Meinzer et al. 1986, Evans et al. 1990) by comparing pressure–volume curves obtained from samples at different levels of initial hydration and found none. The transition point between the nonlinear and linear portions of the curve was taken to be the bulk tissue osmotic potential at zero turgor. Bulk leaf C was determined from the slope of the relationship between relative water content and Ψ_L obtained from pressure–volume curves at values of Ψ_L less negative than $\Psi_{\pi z}$. Values of osmotic potential and C reported here are means from three to five curves per species.

Stem water relations

Moisture release curves for sapwood of terminal branches were determined for ten species according to the method de-

scribed by Meinzer et al. (2003). Briefly, small cylinders of sapwood were allowed to hydrate in distilled water overnight and then quickly blotted to remove excess water, placed in the caps of thermocouple psychrometer chambers (83 Series, JRD Merrill Specialty Equipment, Logan, UT), weighed, and sealed inside the rest of the chamber for determination of Ψ isotherms. Each chamber contained three cylindrical tissue samples. The psychrometer chambers were placed in an insulated water bath and allowed to equilibrate for 2 to 3 h before measurements were started with a 12-channel digital psychrometer meter (85 Series, JRD Merrill Specialty Equipment). Measurements were repeated at 30-min intervals until the Ψ values stabilized. The chambers were opened and the samples were allowed to dehydrate for different time intervals, reweighed in the psychrometer caps, resealed inside the psychrometer chambers and allowed to equilibrate for another determination of Ψ. Moisture release curves were generated by plotting sapwood Ψ against relative water deficit. Data points from three to four replicate curves per species were pooled. Species-specific values of sapwood C (kg m^{-3} MPa^{-1}) were taken as the slopes of linear regressions fitted to the initial phase of moisture release curves plotted as the cumulative mass of water released against sapwood Ψ (Meinzer et al. 2003). Mass of water per unit sapwood volume at saturation (kg m^{-3}) was calculated by multiplying the saturated/dry mass ratio by sapwood density (kg m^{-3}) and subtracting sapwood density. The cumulative mass of water released per unit sapwood volume was then calculated by multiplying the tissue relative water deficit at a given value of sapwood Ψ by the mass of water per unit sapwood volume at saturation. Density was determined for small cylinders of sapwood collected as described above. Volume displacement was determined for samples of saturated tissue, which were oven dried for determination of mass.

Maximum specific conductivity (k_s) was determined for segments of terminal branches 2–5 cm in diameter and greater than 35 cm in length excised near the top of the canopy. After excision, the branches were immediately recut under water in the crane gondola and transported to the laboratory for measurement. In the laboratory, a 15 to17-cm-long section of each branch (0.7 to 1.2 cm in diameter) was cut and both ends were smoothed with clean razor blades. The stem segments were then sealed into a double-ended pressure chamber with both ends protruding and attached with tubing to an apparatus for measuring hydraulic conductivity (k_h). The downstream end of the segment was connected to a 1-ml graduated pipette and the upstream end of the segment was attached to tubing connected to a reservoir of filtered water (0.22 um) that was pressurized at 0.15 MPa for 40 min to remove emboli and restore the segment to its maximum conductivity. The pressure was then lowered to 5.5 kPa and the chamber was pressurized to 0.05 MPa to prevent extrusion of water from leaf scars during measurement of axial flow. When flow had stabilized, the time required for the meniscus in the pipette to cross five consecutive graduation marks (0.5 ml) was recorded. Maximum k_h was calculated as the mass flow rate through the segment divided by the pressure gradient (MPa m^{-1}) across the segment. Conductivity was divided by the xylem cross-sectional area to obtain k_s and by the leaf area distal to the segment to obtain leaf-specific conductivity (k_l). Conductivity data reported here are means of values obtained from five to six stem segments per species. Following conductivity measurements, xylem density was determined as described above.

The water potential of terminal branches (Ψ_{br}) was estimated with a pressure chamber from balance pressures of covered, non-transpiring leaves (Meinzer et al. 2003). Leaves were enclosed in aluminum foil and plastic bags in the afternoon before the day of measurements. At each sampling time, measurements were obtained from three to five leaves of each tree as described above for exposed leaves.

Statistical analysis

Trends in sapwood area-based ETR_{max} and E with ρ_w (Figure 5b) were modeled by first using the regression fitted to the relationship between A_L:A_S and ρ_w ($y = 1.60x - 0.18$; Figure 5a). The corresponding values of A_L:A_S were then used in the regression equations developed for the data in Figures 1 and 2a to obtain values of E ($y = 0.42 + 36.54e^{(-8.96x)}$) and ETR_{max} ($\log(y) = 1.95 - 0.78\log(x)$), which were multiplied by A_L:A_S to convert from a unit leaf area basis to a branch sapwood area basis. These estimates were then normalized to values at a ρ_w of 0.3 g cm^{-3}, which corresponded roughly to the lowest ρ_w among the species studied. Pearson correlations were used to analyze relationships between functional traits and A_L:A_S or ρ_w after log transformation of data. Significance levels of least squares regressions were assessed by ANOVA. Differences in A_L:A_S and ρ_w among sites were evaluated by one-way ANOVA with site as the main factor. Differences in the dependence of sapwood C on ρ_w among sites were assessed by one-way ANCOVA after confirming homogeneity of the regressions for the two sites ($F = 0.64$, $P = 0.45$).

Results

Values of branch A_L:A_S and ρ_w varied widely among the 15 trees studied (Table 1). Branch A_L:A_S was higher at the wetter San Lorenzo site than at the drier and more seasonal Parque Metropolitano ($P = 0.04$). Mean ρ_w was also significantly greater ($P = 0.004$) for the trees studied at the Parque San Lorenzo site. Mean basal diameter and height of the trees selected for study were similar across the two sites. Nine of the 12 leaf and stem functional traits examined were significantly correlated with A_L:A_S or ρ_w across species (Table 2).

Several scaling relationships of leaf functional traits with tree architecture and ρ_w were identified. Transpiration per unit leaf area declined sharply with increasing A_L:A_S for the 12 species in which upper-branch sap flow was measured as a proxy for transpiration (Figure 1). Consistent with the behavior of transpiration, ETR_{max}, an index of photosynthetic capacity, and the ratio of ETR_{max} to leaf N content (ETR_{max}/N), an index of instantaneous photosynthetic nitrogen-use efficiency, also declined with increasing A_L:A_S ($P < 0.0001$ and $P = 0.003$, respectively; Figure 2). The inverse relationship between ETR_{max}/N and A_L:A_S was not associated with significant trends

in leaf N content on a mass or area basis with variation in A_L:A_S or ρ_w (Table 2 and data not shown).

Both midday leaf water potential (Ψ_L) and the bulk leaf osmotic potential at zero turgor ($\Psi_{\pi z}$) declined linearly with increasing ρ_w (P = 0.0003 and 0.004, respectively, Figure 3a). Variation in ρ_w explained about 84% of the variation in Ψ_L. The slopes of the regression lines were not statistically different, implying that minimum values of bulk leaf turgor were similar across species when the daily minimum value of Ψ_L was attained. The specific conductivity of branch sapwood (k_s) decreased exponentially from a maximum value of about 12 kg m^{-1} s^{-1} MPa^{-1} when branch ρ_w was 0.4 g cm^{-3} to a minimum value of 1.6 kg m^{-1} s^{-1} MPa^{-1} when ρ_w was 0.74 g cm^{-3} (Figure 3b). Species from both sites appeared to share a common relationship between k_s and ρ_w. However, k_s was not significantly correlated with A_L:A_S (Table 2). Consistent with the relationship between k_s and ρ_w, k_l decreased exponentially with ρ_w (Figure 3c). Sapwood C also declined sharply with increasing ρ_w (Figure 4a), but distinct site-specific relationships appeared to exist with species occurring at the wetter forest site having greater values of sapwood C at a given value of ρ_w (F = 40.6, P = 0.0004). Maximum values of C were similar (~400 kg m^{-3} MPa^{-1}) at both sites. Bulk leaf C on a mass basis was inversely related to ρ_w (P = 0.004) with species from both sites appearing to share a common relationship (Figure 4b).

The leaf area to sapwood area ratio of upper-canopy branches increased about threefold with a doubling of ρ_w (Figure 5a). Although a single linear regression fitted to data from both sites was highly significant (r^2 = 0.66, P = 0.0002), the re-

Table 2. Correlation coefficients and their statistical significance for comparisons of leaf and stem functional traits with branch architecture and sapwood density. Traits with negative values (Ψ_{br}, Ψ_L, $\Psi_{\pi z}$) were converted to positive values for log transformation, but signs of correlation coefficients reflect correlations for untransformed data. Abbreviations: * P < 0.05, ** P < 0.01, *** P < 0.001.

Trait	n	A_L:A_S	Wood density
Leaf			
E_{max}	12	−0.82 ***	−0.47 ***
ETR_{max}	10	−0.97 ***	−0.62
ETR/N	10	−0.83 **	−0.64 *
%N	15	0.20	0.41
LMA	15	0.21	0.51 *
Ψ_L	9	−0.51	−0.93 ***
$\Psi_{\pi z}$	9	−0.22	−0.85 **
C	9	−0.58	−0.93 ***
Stem			
k_s	10	−0.46	−0.83 **
k_l	10	−0.67 *	−0.89 ***
Ψ_{br}	10	−0.30	−0.38
C	10	0.04	−0.40

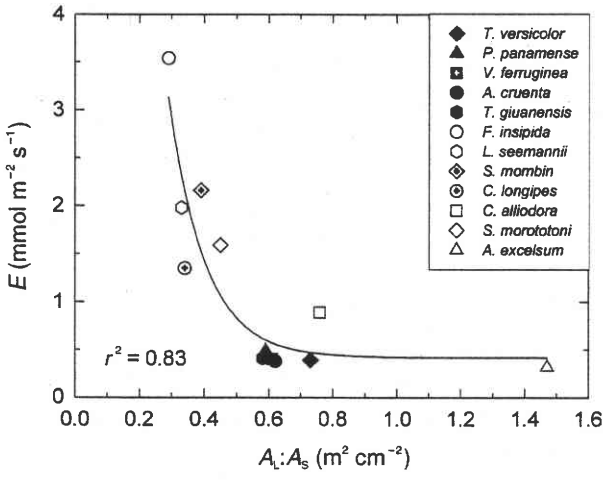

Figure 1. Maximum branch transpiration rate per unit leaf area (E) in relation to leaf area:sapwood area ratio (A_L:A_S) for upper crown branches of 12 Panamanian forest tree species growing in two sites with different rainfall regimes and forest types. Values are means of three to five branches per tree. Open symbols, drier site; closed symbols wetter site.

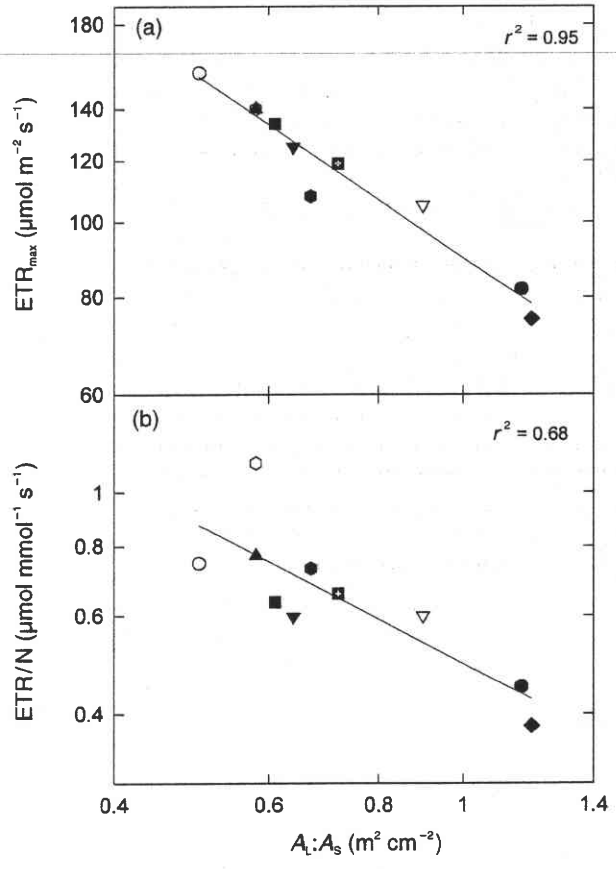

Figure 2. Log–log plots of (a) maximum photosynthetic electron transport rate per unit leaf area (ETR_{max}) and (b) maximum electron transport rate per unit leaf nitrogen (ETR/N) in relation to the branch leaf area:sapwood area ratio (A_L:A_S) for 10 Panamanian forest tree species. Symbols: (▽) *Chrysophllum cainito*, (■) *Manilkara bidentata*, (▼) *Trattinickia aspera*, remaining symbols as in Figure 1.

lationship for the trees studied at the drier Parque Metropolitano site was much less variable (r^2 = 0.97, P < 0.0001). Scaling of transpiration on a unit branch sapwood area basis with ρ_w reduced transpiration by about 20% over the range of ρ_w observed (Figure 5b). In contrast, scaling photosynthetic capacity (ETR_{max}) per branch sapwood area increased photosynthetic capacity by about 30% over the same range of ρ_w (Figure 5b). The total amount of foliar N per unit sapwood area increased from ~60 mmol N cm^{-2} sapwood area in the species with the lowest ρ_w to ~210 mmol N cm^{-2} in the species with the highest ρ_w (P = 0.0004, Figure 5c).

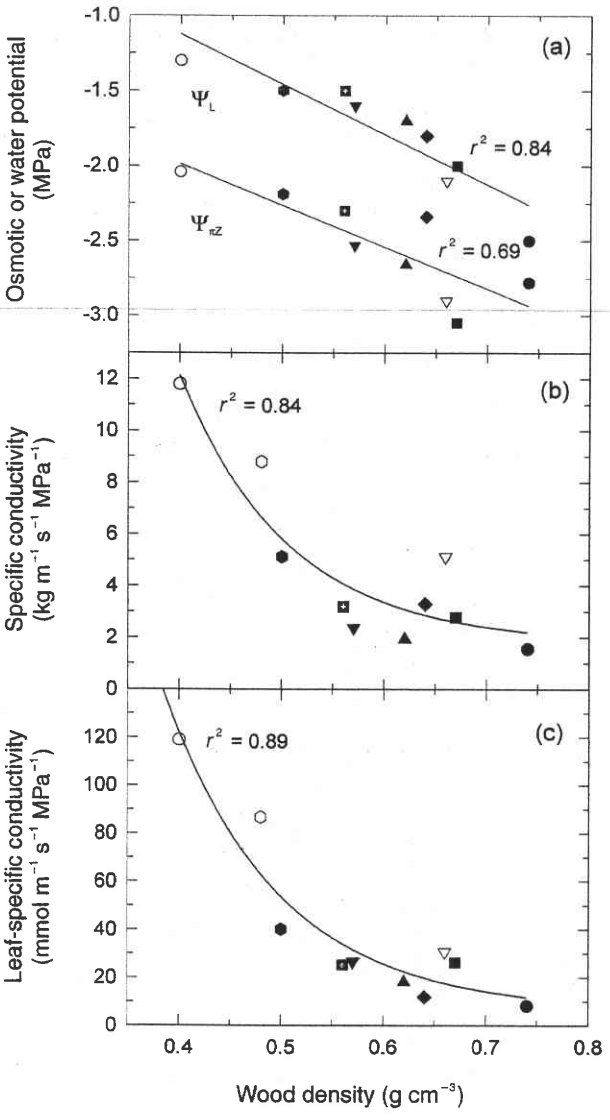

Figure 3. Leaf and stem functional traits in relation to branch wood density for Panamanian forest trees. (a) Mean daily minimum leaf water potential (Ψ_L) and bulk leaf osmotic potential at zero turgor ($\Psi_{\pi Z}$) for nine species, (b) branch xylem specific conductivity for 10 species, (c) leaf-specific conductivity for the same species shown in (b). Symbols as in Figures 1 and 2.

Discussion

Simple tree architectural and wood physical properties (A_L:A_S and ρ_w) accounted for a large fraction of the variation in several leaf and stem functional traits among individuals and species growing at contrasting sites. As hypothesized, A_L:A_S appeared to be a reliable proxy for K_l, and ρ_w served as a proxy for k_s, C and their impact on leaf water relations. The scaling relationships found here have practical and theoretical implications for understanding and predicting emergent properties of complex multi-species ecosystems. These relationships obtained from data collected over multiple years on individuals growing in contrasting sites and representing different tree functional groups, are unlikely to be merely correlative, but imply direct or indirect mechanistic links between variables as we argue below.

Branch architectural constraints on leaf gas exchange

As a relative index of potential transpirational demand in relation to the hydraulic capacity of the xylem, A_L:A_S is an important component of tree hydraulic architecture. Results of a number of studies suggest that k_l scales uniformly with A_L:A_S among co-occurring species with A_L:A_S explaining 50% or more of the variation in k_l (Tausend et al. 2000, Bucci et al. 2005). Furthermore, adjustments in A_L:A_S have been shown to

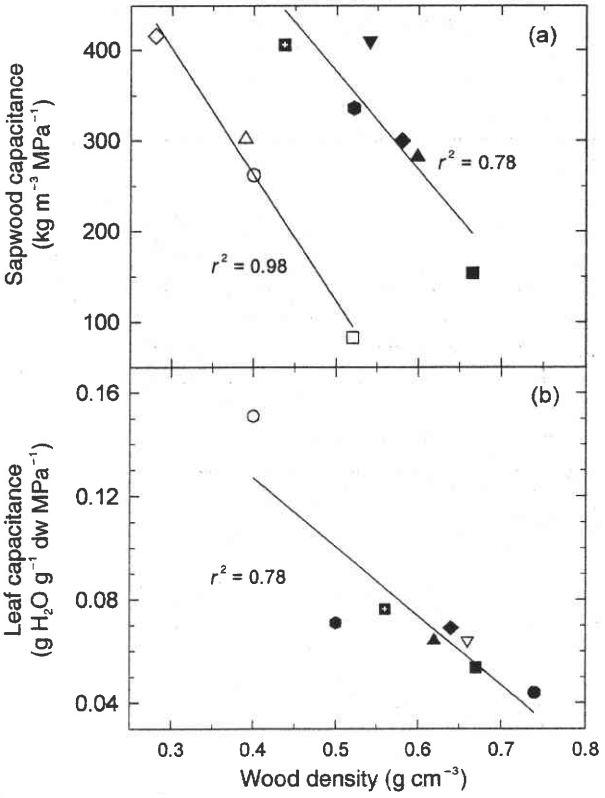

Figure 4. (a) Sapwood and (b) leaf capacitance in relation to wood density for several Panamanian forest tree species. Symbols as in Figures 1 and 2.